AIP | The Journal of Chemical Physics

A broadened classical master equation approach for nonadiabatic dynamics at metal surfaces: Beyond the weak molecule-metal coupling limit

Wenjie Dou and Joseph E. Subotnik

Citation: The Journal of Chemical Physics **144**, 024116 (2016); doi: 10.1063/1.4939734
View online: http://dx.doi.org/10.1063/1.4939734
View Table of Contents: http://scitation.aip.org/content/aip/journal/jcp/144/2?ver=pdfcov
Published by the AIP Publishing

A broadened classical master equation approach for nonadiabatic dynamics at metal surfaces: Beyond the weak molecule-metal coupling limit

Wenjie Dou and Joseph E. Subotnik
Department of Chemistry, University of Pennsylvania, Philadelphia, Pennsylvania 19104, USA

(Received 2 November 2015; accepted 29 December 2015; published online 13 January 2016)

A broadened classical master equation (BCME) is proposed for modeling nonadiabatic dynamics for molecules near metal surfaces over a wide range of parameter values and with arbitrary initial conditions. Compared with a standard classical master equation–which is valid in the limit of weak molecule-metal couplings–this BCME should be valid for both weak and strong molecule-metal couplings. (The BCME can be mapped to a Fokker-Planck equation that captures level broadening correctly.) Finally, our BCME can be solved with a simple surface hopping algorithm; numerical tests of equilibrium and dynamical observables look very promising. © *2016 AIP Publishing LLC*. [http://dx.doi.org/10.1063/1.4939734]

I. INTRODUCTION

The dynamics of molecules near metal surfaces are often nonadiabatic, i.e., the dynamics do not obey the Born-Oppenheimer approximation.[1] In such a case, just as for problems in photochemistry, there are several energy scales that are relevant. Consider, for example, the Anderson-Holstein (AH) model (Eqs. (1)-(4)), which is the simplest model Hamiltonian for describing such dynamics. The Anderson-Holstein model (and generalizations thereof) has been broadly used to describe molecular junctions,[2–4] quantum dots,[5–7] gas scattering from metals,[8–10] and electrochemical systems.[11] For the AH model, we consider an impurity energy level coupled both to a manifold of electronic states representing the metal and also to a single nuclear degree of freedom.[12,13] There are at least three important energy scales for the AH Hamiltonian: the inverse time scale for nuclear motion ω, the strength of the molecule-metal coupling Γ, and the temperature of the metal T.[14] In general, propagating dynamics for the simple AH model with an arbitrary set of parameter values to convergence can be difficult for numerically exact methods, such as Numerical Renormalization Group,[15–17] Multi-Configuration Time-Dependent Hartree,[18] and Path Integral Monte Carlo.[19] Thus, if we seek an algorithm to describe more complicated, realistic systems beyond the AH model, appropriate approximations must be made.

For this paper, we restrict ourselves to the case $kT > \hbar\omega$, where a classical description of the nuclear motion should be feasible. Even for this regime, however, no simple solution is available. For example, in the literature, we find two different approaches for further simplifying the AH model, each based on the strength of electron-metal coupling (Γ) (see Fig. 1). On the one hand, for small Γ, a perturbative treatment leads to a variety of master equations,[20–25] where usually the level broadening is disregarded; for the most part, these approaches are valid only when the electron-metal coupling is small compared to temperature ($\Gamma < kT$). On the other hand, in the limit of large Γ, an adiabatic approach yields a broadened Fokker-Planck (BFP) equation, or equivalently Langevin dynamics on a broadened potential of mean force.[26–29] As usual, the adiabatic approximation requires that the nuclear dynamics be slow compared to electron-metal coupling, roughly $\Gamma > \hbar\omega$; the adiabatic approximation also cannot be used in a straightforward formalism for short times if the system begins out of equilibrium.

In a series of recent papers,[20,23,30] we have now started to analyze both of the approaches above. Almost a year ago, in Refs. 20 and 23, we followed the first approach above and studied a classical master equation (CME) to model nonadiabatic dynamics near metal surfaces in the limit $\Gamma < kT$. This CME did not include broadening. More recently, in Ref. 30, we considered our CME in the further limit that $\Gamma > \hbar\omega$, and we showed that our CME can be mapped to a Fokker-Planck (FP) equation (where the nuclei move on the potential of mean force with random force and experience frictional damping from the electronic degrees of freedom). Most importantly, in Ref. 30, we also showed that our FP equation is equivalent to the BFP equation derived by von Oppen and co-workers in the limit of high temperature.[26] It must be emphasized that von Oppen and co-workers derived their BFP equation using the second approach listed above, i.e., assuming only that $\Gamma > \hbar\omega$ (and not requiring that $\Gamma < kT$). Thus, for low temperature, the von Oppen BFP equation includes broadening whereas our FP equation does not.

With this background in mind, in the present paper, we will argue that it is possible to bridge the small and large Γ cases above by extrapolation. While a rigorous approach for connecting these two limits was recently proposed by Galperin and Nitzan,[31] we will propose a practical approach by ansatz. To make this connection, we will modify our CME to incorporate level broadening, and we will refer to the resulting equation (see below) as a "broadened classical master equation (BCME)." In the limit that $\Gamma < kT$, our BCME reduces to the unbroadened CME; in the limit that $\Gamma > \hbar\omega$, our BCME can be mapped to von Oppen's BFP equation. Therefore, we would hope that our BCME should be valid for all Γ (see Fig. 1), so long as the nuclei are

Methods	Eqs.	Refs.
Fokker-Planck (FP)	14, 17, 18	Dou *et al* [30]
broadened Fokker-Planck (BFP)	21, 22, A1	von Oppen *et al* [26]
classical master equation (CME)	6-7	Dou *et al* [20] von Oppen *et al* [21]
broadened classical master equation (BCME)	23-24	

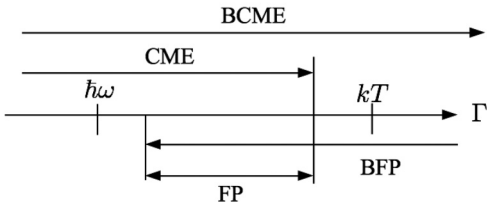

FIG. 1. The energy regimes for different theoretical approaches. All methods treat the nuclei classically, hence $kT > \hbar\omega$. Depending on how strong the electron-metal coupling (Γ) is, different methods will be applicable. A broadened CME (BCME) will have the largest range of applicability, connecting the domains of the standard CME and broadened FP (BFP) equation.

classical, $kT > \hbar\omega$. Note that such an approach would be key for two important applications. First, with such an approach, we would be able to study the photoinduced dynamics of molecules near strongly coupled metal surfaces; recall that von Oppen's BFP equation assumes that the nuclei must begin and remain in quasi-equilibrium with the electronic degrees of freedom so that out of equilibrium initial conditions are not permitted. Second, for many reactions on surfaces, the molecule-metal coupling changes strongly with position (x), where x might be the distance to the metal surface. In such a case, if Γ is not a constant, one cannot assume that $\Gamma(x) < kT$ or $\Gamma(x) > \hbar\omega$. With an accurately BCME, however, one should be able to treat both cases so that one can model inner sphere electrochemical reactions occurring at surfaces.

Before concluding this introduction, we note that the BCME presented below can be solved numerically with a simple, stable surface hopping (SH) procedure. Compared with our previous SH algorithm[20] without broadening, there is now one difference: whereas all jumps between potential energy surfaces are local in phase space for the standard CME, momentum adjustments become necessary for the BCME. Of course, momentum jumps also occur in Tully's fewest-switches surface hopping algorithm.[32] Thus, one must wonder whether in the future we will find additional connections between our BCME and Tully style surface hopping; this theme will be explored in a future article.

An outline of this article is as follows. In Sec. II, we present a BCME that incorporates level broadening. In Sec. III we describe the surface hopping algorithm to solve the BCME. In Sec. IV, we show results. We conclude in Sec. V.

II. THEORY

For simplicity, we now discuss the Anderson-Holstein (AH) model, which is the simplest possible model for describing coupled nuclear electronic motion near a metal surface. (A more general discussion of our algorithm is given in Appendix B, where we consider the case of arbitrary potential energy surfaces and many nuclear degrees of freedom.) The AH Hamiltonian is

$$H = H_s + H_b + H_c, \tag{1}$$

$$H_s = E(x)d^+d + \frac{1}{2}\hbar\omega(x^2 + p^2), \tag{2}$$

$$H_b = \sum\nolimits_k (\epsilon_k - \mu)c_k^+ c_k, \tag{3}$$

$$H_c = \sum\nolimits_k V_k(c_k^+ d + d^+ c_k), \tag{4}$$

where the energy difference between diabats is defined as

$$E(x) \equiv \sqrt{2}gx + E_d. \tag{5}$$

Here, we find an impurity electronic energy level (with creation operator d^+ and annihilation operator d) coupled both to a manifold of electrons (c_k^+, c_k labeled by Bloch state k) and a nuclear degree of freedom (x, p). We use dimensionless x and p coordinates. In Eq. (5), g describes the strength of electron-phonon coupling ($\sqrt{2}$ is a factor used by convention). μ is the Fermi energy of the electronic bath.

A. Standard classical master equation

In a classical master equation (CME) approach, we use probability density $P_0(x,p,t)$ ($P_1(x,p,t)$) to describe a state with the impurity being unoccupied (occupied), and the oscillator being at position x with momentum p. When $\Gamma \ll kT$, the time evolution of the probability density is given by[20,21]

$$\begin{aligned}\hbar\frac{\partial P_0(x,p,t)}{\partial t} &= -\hbar\omega p\frac{\partial P_0(x,p,t)}{\partial x} + \hbar\omega x\frac{\partial P_0(x,p,t)}{\partial p}\\ &\quad - \Gamma f(E(x))P_0(x,p,t)\\ &\quad + \Gamma(1 - f(E(x)))P_1(x,p,t),\end{aligned} \tag{6}$$

$$\begin{aligned}\hbar\frac{\partial P_1(x,p,t)}{\partial t} &= -\hbar\omega p\frac{\partial P_1(x,p,t)}{\partial x}\\ &\quad + (\hbar\omega x + \sqrt{2}g)\frac{\partial P_1(x,p,t)}{\partial p}\\ &\quad + \Gamma f(E(x))P_0(x,p,t)\\ &\quad - \Gamma(1 - f(E(x)))P_1(x,p,t).\end{aligned} \tag{7}$$

Here, Γ is the hybridization function that describes the strength of electron-metal coupling, and we assume Γ is a constant (i.e., the wide band approximation), $\Gamma(\epsilon) = 2\pi\sum_k |V_k|^2\delta(\epsilon - \epsilon_k) \equiv \Gamma$. $f(E(x)) = \frac{1}{e^{E(x)/kT}+1}$ is a Fermi function.

Eqs. (6) and (7) have a simple physical picture: motion along two diabatic potential surfaces (with a timescale of $1/\omega$), plus hopping (with a timescale of $\hbar/\Gamma$) between $P_0(x,p,t)$ and $P_1(x,p,t)$. The two diabatic potential surfaces are

$$V_{diab}^0 = \frac{1}{2}\hbar\omega x^2, \tag{8}$$

$$V_{diab}^1 = \frac{1}{2}\hbar\omega x^2 + \sqrt{2}gx + E_d. \tag{9}$$

Following Ref. 30, we can define new densities $A(x,p,t)$ and $B(x,p,t)$ according to

$$P_0(x,p,t) = (1 - f(E(x)))A(x,p,t) + B(x,p,t), \tag{10}$$

$$P_1(x,p,t) = f(E(x))A(x,p,t) - B(x,p,t). \tag{11}$$

Plugging Eqs. (10) and (11) into Eqs. (6) and (7), we arrive at

$$\hbar\frac{\partial A(x,p,t)}{\partial t} = -\hbar\omega p\frac{\partial A(x,p,t)}{\partial x} + (\hbar\omega x + \sqrt{2}gf(E(x)))\frac{\partial A(x,p,t)}{\partial p} - \sqrt{2}g\frac{\partial B(x,p,t)}{\partial p}, \tag{12}$$

$$\hbar\frac{\partial B(x,p,t)}{\partial t} = -\hbar\omega p\frac{\partial B(x,p,t)}{\partial x} + (\hbar\omega x + \sqrt{2}g - \sqrt{2}gf(E(x)))\frac{\partial B(x,p,t)}{\partial p} - \Gamma B(x,p,t)$$
$$- \sqrt{2}gf(E(x))(1-f(E(x)))\frac{\partial A(x,p,t)}{\partial p} + \hbar\omega\frac{\partial f(E(x))}{\partial x}pA(x,p,t). \tag{13}$$

Now, we see $A(x,p,t)$ and $B(x,p,t)$ are moving on two different potential surfaces, which we will refer to as adiabatic potential surfaces

$$V^0_{adiab} = \frac{1}{2}\hbar\omega x^2 + \sqrt{2}g\int_{x_0}^{x} f(E(x'))dx', \tag{14}$$

$$V^1_{adiab} = \frac{1}{2}\hbar\omega x^2 + \sqrt{2}g\int_{x_0}^{x} (1-f(E(x')))dx'. \tag{15}$$

As explained in Ref. 30, if $\Gamma > \hbar\omega$—such that $B(x,p,t)$ is small compared with $A(x,p,t)$ and such that $B(x,p,t)$ changes slowly with respect to x,p,t—we can approximate Eq. (13) by

$$\Gamma B(x,p,t) = -\sqrt{2}gf(E(x))(1-f(E(x)))\frac{\partial A(x,p,t)}{\partial p} + \hbar\omega\frac{\partial f(E(x))}{\partial x}pA(x,p,t). \tag{16}$$

If we plug Eq. (16) back into Eq. (12), we get a FP equation (we have used $\frac{\partial f(E(x))}{\partial x} = -\sqrt{2}gf(E(x))(1-f(E(x)))\frac{1}{kT}$),

$$\hbar\frac{\partial A(x,p,t)}{\partial t} = -\hbar\omega p\frac{\partial A(x,p,t)}{\partial x} + \frac{\partial V^0_{adiab}}{\partial x}\frac{\partial A(x,p,t)}{\partial p} + \hbar\gamma_e(x)\frac{\partial}{\partial p}(pA(x,p,t)) + \hbar\gamma_e(x)\frac{kT}{\hbar\omega}\frac{\partial^2 A(x,p,t)}{\partial p^2}, \tag{17}$$

where $\gamma_e(x)$ is the electronic friction,

$$\gamma_e(x) = \frac{2g^2}{\Gamma}\frac{\omega}{kT}f(E(x))(1-f(E(x))). \tag{18}$$

B. The incorporation of broadening

To incorporate level broadening, we propose replacing $f(E(x))$ in Eq. (12) by $n(E(x))$,

$$\hbar\frac{\partial A(x,p,t)}{\partial t} = -\hbar\omega p\frac{\partial A(x,p,t)}{\partial x} + (\hbar\omega x + \sqrt{2}gn(E(x)))\frac{\partial A(x,p,t)}{\partial p} - \sqrt{2}g\frac{\partial B(x,p,t)}{\partial p}, \tag{19}$$

where $n(Z)$ is defined as

$$n(Z) = \int\frac{d\epsilon}{2\pi}\frac{\Gamma}{(\epsilon - Z)^2 + (\Gamma/2)^2}f(\epsilon). \tag{20}$$

If we plug Eq. (16) back into Eq. (19), we get

$$\hbar\frac{\partial A(x,p,t)}{\partial t} = -\hbar\omega p\frac{\partial A(x,p,t)}{\partial x} + \frac{\partial\tilde{V}^0_{adia}}{\partial x}\frac{\partial A(x,p,t)}{\partial p} + \hbar\gamma_e(x)\frac{\partial}{\partial p}(pA(x,p,t)) + \hbar\gamma_e(x)\frac{kT}{\hbar\omega}\frac{\partial^2 A(x,p,t)}{\partial p^2}. \tag{21}$$

Here, $\tilde{V}^0_{adia}$ is the (broadened) potential of mean force, which we also refer to as the broadened adiabatic potential surface 0 compared with the unbroadened adiabatic potential surface 0 in Eq. (14)

$$\frac{\partial\tilde{V}^0_{adia}}{\partial x} = \hbar\omega x + \sqrt{2}gn(E(x)). \tag{22}$$

Finally, if we use Eqs. (10) and (11) to calculate P_0 and P_1 from Eqs. (13) and (19), we find

$$\hbar\frac{\partial P_0(x,p,t)}{\partial t} = -\hbar\omega p\frac{\partial P_0(x,p,t)}{\partial x} + \hbar\omega x\frac{\partial P_0(x,p,t)}{\partial p} - \Gamma f(E(x))P_0(x,p,t) + \Gamma(1-f(E(x)))P_1(x,p,t)$$
$$+ \sqrt{2}g(n(E(x)) - f(E(x)))(1-f(E(x)))\frac{\partial\big(P_0(x,p,t) + P_1(x,p,t)\big)}{\partial p}, \tag{23}$$

$$\hbar\frac{\partial P_1(x,p,t)}{\partial t} = -\hbar\omega p\frac{\partial P_1(x,p,t)}{\partial x} + (\hbar\omega x + \sqrt{2}g)\frac{\partial P_1(x,p,t)}{\partial p} + \Gamma f(E(x))P_0(x,p,t) - \Gamma(1-f(E(x)))P_1(x,p,t)$$
$$+ \sqrt{2}g(n(E(x)) - f(E(x)))f(E(x))\frac{\partial\big(P_0(x,p,t) + P_1(x,p,t)\big)}{\partial p}. \tag{24}$$

Henceforward, we will refer to the set of Equations (23) and (24) as one BCME. Several comments must now be made.

- Compared with the original CME (Eqs. (6) and (7)), one finds new terms in the BCME proportional to $\frac{\partial\left(P_0(x,p,t)+P_1(x,p,t)\right)}{\partial p}$. Interestingly, these new terms correspond not only to modified forces, but also to dynamical momentum jumps (which are also present in the usual, Tully style surface hopping algorithm[32] for molecular photochemistry).
- In the limit of small Γ, i.e., $\Gamma \ll kT$, level broadening can be disregarded and $n(E(x)) \approx f(E(x))$. Thus, in this case, the BCME obviously reduces to the original CME (Eqs. (6) and (7)).
- In the limit of large Γ, where we can make an adiabatic approximation if $\Gamma \gg \hbar\omega$, the potential of mean force in Eq. (22) agrees exactly with the work of von Oppen *et al.*: the potential of mean force is broadened (i.e., $f(E(x))$ is replaced by $n(E(x))$).
- Regarding the definition of electronic friction $\gamma_e(x)$, Eq. (18) agrees only partially with the work von Oppen *et al.*[26] Whereas we invoke a frictional damping value without broadening (i.e., the raw Fermi function appears in Eq. (18)), von Oppen *et al.* derive a damping term with broadening. See Eq. (A1). Both frictional terms will be identical in the limit of large temperature, $\Gamma \ll kT$.

  In practice, our BCME (Eqs. (23) and (24)) can be further corrected to account for a broadened frictional damping term; see Appendix A. For most problems, such a broadened correction for the friction is small (Eq. (A1) versus Eq. (18)) relative to the broadened correction for potential of mean force (Eq. (22) versus Eq. (14)). Below, we do not include such corrections in our discussion of a surface hopping algorithm.

III. MODIFIED SURFACE HOPPING PROCEDURE

We use a modified surface hopping (SH) procedure to solve the BCME (Eqs. (23) and (24)). As in any Monte Carlo algorithm, we use a swarm of trajectories to sample the probability densities.[20,32] The modified SH algorithm is as simple as the following.

1. We initialize the positions, momenta and active surface for each trajectory. In this paper, we will usually prepare our initial state in the following distribution (unless stated otherwise):

$$P_1(x,p,0) = C\exp\Big(-\frac{1}{2}\hbar\omega(x-x_1)^2/kT_i - \frac{1}{2}\hbar\omega p^2/kT_i\Big), \tag{25}$$

$$P_0(x,p,0) = 0, \tag{26}$$

such that $N \equiv \int dxdp\, P_1(x,p,0) = 1$. The constant $x_1 \equiv -\sqrt{2}g/\hbar\omega$ is the center of potential surface 1. T_i is some initial temperature that can be different from the temperature of the electronic bath. C is a normalization factor.

2. For each trajectory, suppose the active potential surface is 1 [or 0]. At each time step, we generate a random number ξ from 0 to 1. If $\xi > \Gamma(1-f(E(x)))dt$ [$\xi > \Gamma f(E(x))dt$], the oscillator continues to move along potential surface 1 [surface 0] for a time step dt. The force felt by the oscillator on surface 1 is

$$F_1 \equiv \frac{d\tilde{V}^1_{diab}}{dx} = -\hbar\omega(x-x_1) - \sqrt{2}g(n(E(x)) - f(E(x)))f(E(x)), \tag{27}$$

and the force felt on surface 0 is

$$F_0 \equiv \frac{d\tilde{V}^0_{diab}}{dx} = -\hbar\omega x - \sqrt{2}g(n(E(x)) - f(E(x)))(1-f(E(x))). \tag{28}$$

We refer to the corresponding potentials as broadened diabatic potential surfaces $\tilde{V}^\alpha_{diab} = \int_{x_0}^{x} F_\alpha dx'$, $\alpha = 0,1$.
3. if $\xi < \Gamma(1-f(E(x)))dt$ [$\xi < \Gamma f(E(x))dt$], the oscillator hops to the potential surface 0 [surface 1]. When the oscillator hops, the momentum changes by

$$\Delta p = -\sqrt{2}g(n(E(x)) - f(E(x)))/\Gamma, \tag{29}$$

while the position remains unchanged. This momentum adjustment always pushes the particle in the direction of the crossing. Thereafter, the trajectory moves along its new surface for the next time step dt.
4. We repeat steps 2-3 for all trajectories until we reach the desired time slice.

Now, to calculate observables, we will define new densities,

$$\begin{aligned}\tilde{P}_0(x,p,t) &= (1-n(E(x)))A(x,p,t) + B(x,p,t) \\ &\quad + (n(E(x)) - f(E(x)))A(x,p,t) \\ &\quad \times \exp(-\int_0^t dt\, \Gamma(x(t))),\end{aligned} \tag{30}$$

$$\begin{aligned}\tilde{P}_1(x,p,t) &= n(E(x))A(x,p,t) - B(x,p,t) \\ &\quad - (n(E(x)) - f(E(x)))A(x,p,t) \\ &\quad \times \exp(-\int_0^t dt\, \Gamma(x(t))).\end{aligned} \tag{31}$$

Initially, at time zero, by construction we have $\tilde{P}_\alpha = P_\alpha$ ($\alpha = 0,1$). Afterwards, at longer times, both the second and third term (in the above equations) will decay, so that

$$\tilde{P}_0(x,p,t) \to (1-n(E(x)))A(x,p,t), \tag{32}$$

$$\tilde{P}_1(x,p,t) \to n(E(x))A(x,p,t). \tag{33}$$

Thus, it is obviously true that our algorithm will find the correct long time electronic population,[33]

$$N = \int dxdp\, \tilde{P}_1(x,p,t) \xrightarrow{\Gamma t \gg 1} \int dxdp\, n(E(x))A(x,p,t). \tag{34}$$

IV. RESULTS

A. Potential energy surfaces

Before considering dynamics, we study the different potential surfaces (broadened and unbroadened). Because broadened diabatic potentials are defined only up to a constant, we fix the minimum of each potential to have value $V(x)_{min} = 0$.

From Fig. 2, we notice that, by incorporating level broadening, the barrier between wells along the potential of mean force is lowered significantly, and the crossing point between diabats is similarly lowered. Furthermore, even though the broadened diabatic potential surfaces can be shifted from the unbroadened diabatic surfaces asymptotically, the two quantities will predict identical forces far from the crossing region. Finally, to convince the reader that our SH solution to the BCME with momentum jumps is accurate, in Fig. 2, we also plot minus the log of the position distribution of the oscillator (times kT) from SH trajectories, $-kT\ln(A)$. This quantity agrees with the broadened potential of mean force very well, indicating that our SH procedure does capture the correct equilibrium distribution.

B. Electronic dynamics

We now turn to dynamics, and we begin with electronic properties. In Fig. 3, we plot the electronic population (N) as a function of time for the different theoretical approaches. Here, Γ is larger than kT, $\Gamma = 2kT \approx 6\hbar\omega$. To estimate an electronic population with an unbroadened FP equation, we average the Fermi function $f(E(x(t)))$ over simulation trajectories $x(t)$;[30] for a broadened BFP equation, we average the function $n(E(x(t)))$ where n is defined in Eq. (20).

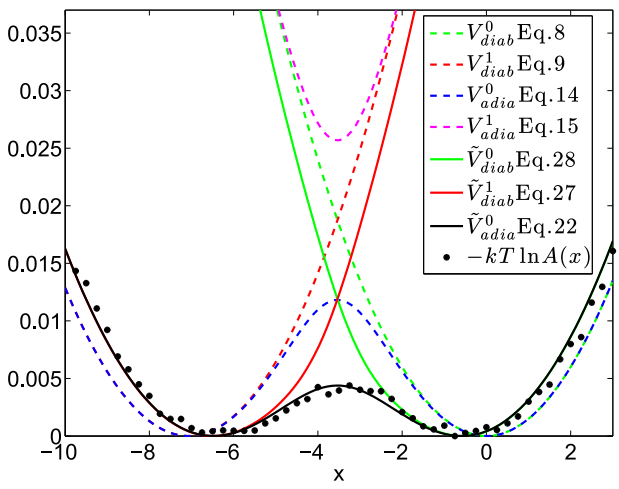

FIG. 2. Potential surfaces (diabatic and adiabatic, with and without broadening) for the AH model. $\hbar\omega = 0.003$, $g = 0.015$, $\Gamma = 0.03$, $kT = 0.01$, $\bar{E}_d = 0$ ($\bar{E}_d \equiv E_d - g^2/\hbar\omega$ is the renormalized energy level). We also plot minus the log of equilibrium total density, $-kT\ln(A)$, $A(x) = \int dp(P_0(x,p) + P_1(x,p))$ from surface hopping simulation (black dots); the latter quantity agrees with the broadened potential of mean force $\tilde{V}^0_{adia}$ very well. Diabat 1 corresponds to the molecular level being occupied. Diabat 0 corresponds to the molecular level being unoccupied.

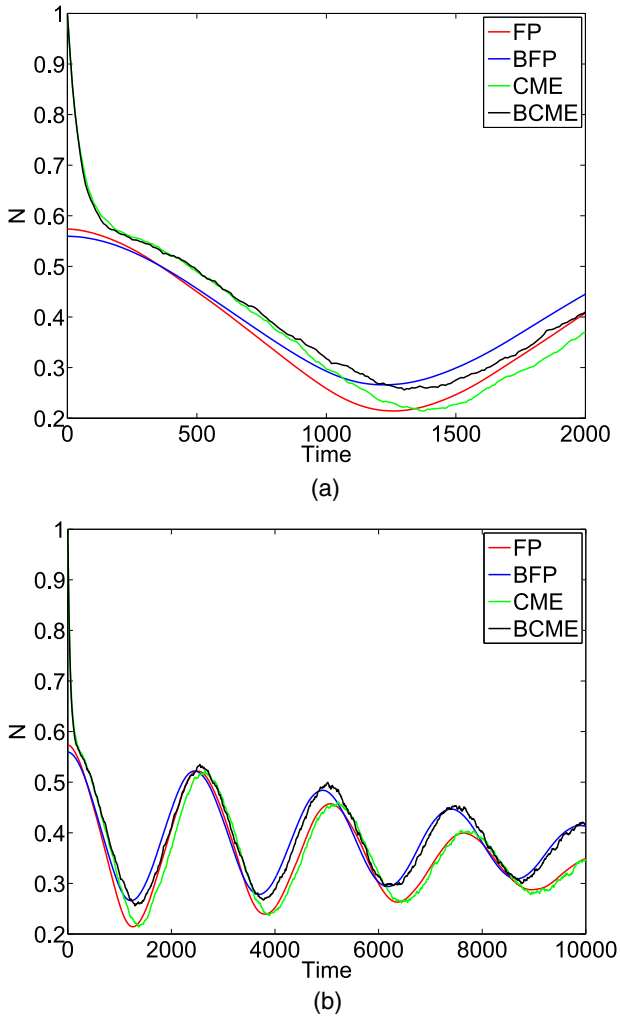

FIG. 3. Electronic population as a function of (a) shorter time (b) longer time: $\Gamma = 0.02$, $\omega = 0.003$, $g = 0.0075$, $kT = 0.01$, $\bar{E}_d = 0.01$ ($\bar{E}_d \equiv E_d - g^2/\hbar\omega$ is the renormalized energy level). We set $\hbar = 1$. We prepare the initial temperature as $T_i = 5T$ for symmetry with Fig. 4. For notation, FP = Fokker-Planck (unbroadened), BFP = broadened Fokker-Planck, CME = classical master equation (unbroadened), BCME=broadened classical master equation. See Fig. 1. Note that the BCME results agree with CME at short time and BFP at long time, as one would hope.

From Fig. 3, we find that, on the one hand, at long times, the BCME/SH results agree with BFP results. Thus, our BCME approach does recover the correct long time equilibrium population (on a broadened surface). Note that, at long times, our broadened results do not agree with the unbroadened results. Thus, for such a large Γ, broadening the potential energy surface will clearly be important for dynamics. At short times, on the other hand, we note that BCME/SH results agree with unbroadened CME/SH results and disagree with BFP results. As discussed earlier and in Ref. 30, all FP equations (broadened or unbroadened) cannot be trusted at very early times if the simulation does not start from near equilibrium. In this case, because of the inevitable mixing of surfaces, the FP approaches cannot even recover the correct initial electronic population at time zero ($N = 1$).[30]

In the end, only a BCME approach is reliable in the short and long time limits.

C. Nuclear dynamics

Finally, we consider nuclear dynamics and begin by plotting the kinetic energy of the oscillator in Fig. 4. As should be expected, when Γ is less than or nearly equal to kT, $\Gamma \leq kT$, Fig. 4(a) shows that the level broadening does not affect the real time dynamics. Fig. 4(a) also shows that, when $\Gamma < \hbar\omega$, the CME and FP methods do not agree with each other. As shown in Fig. 4(b), the CME and FP methods agree only for large Γ, $\Gamma \gg \hbar\omega$, where the adiabatic approximation is valid.

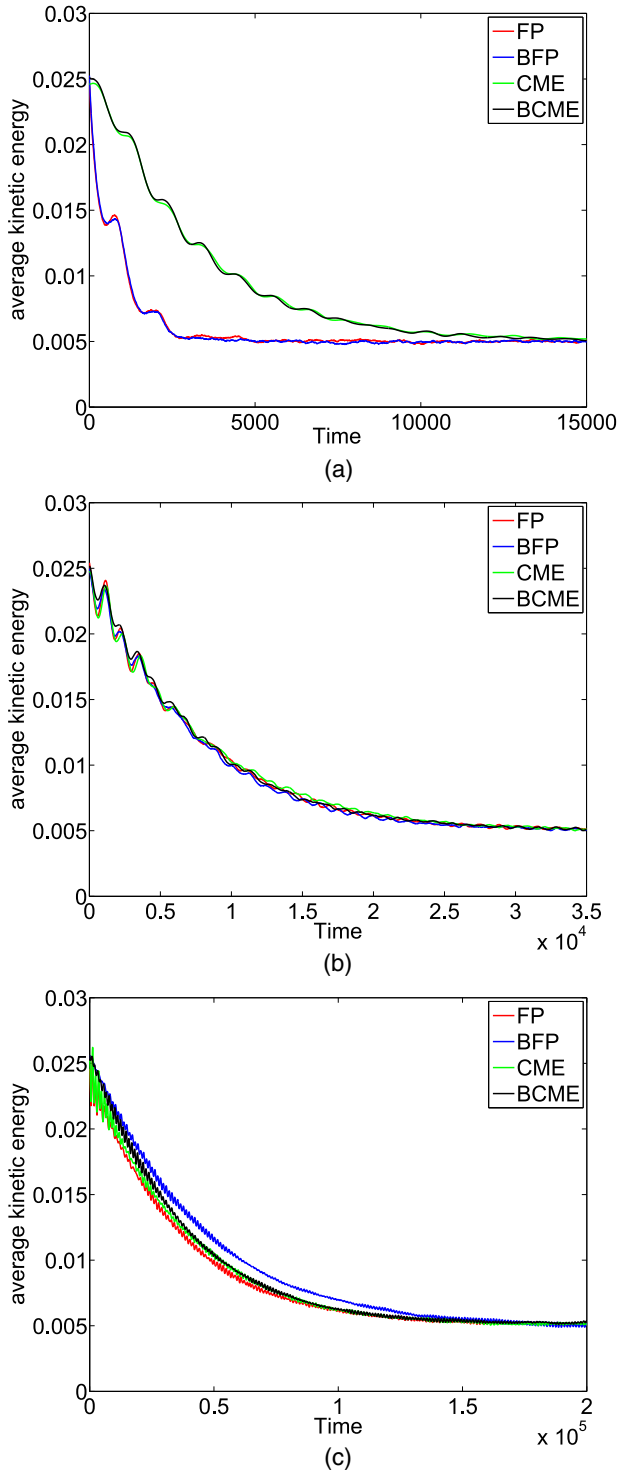

FIG. 4. Average kinetic energy as a function of real time: $\omega = 0.003$, $g = 0.0075$, $kT = 0.01$, $\bar{E}_d = 0.01$ ($\bar{E}_d \equiv E_d - g^2/\hbar\omega$ is the renormalized energy level). We set $\hbar = 1$. We prepare the initial temperature as $T_i = 5T$. Note that the BCME agrees with the CME for small Γ. Same notation as in Fig. 1. (a) $\Gamma = 0.002$. (b) $\Gamma = 0.02$. (c) $\Gamma = 0.1$.

Next, consider the case where $\Gamma \gg kT$. Here, one might expect to find large signature of broadening. However, even for very large Γ, the average kinetic energy does not seem to be very different with or without broadening, as shown in Fig. 4(c). Thus, the average kinetic energy would not appear to be the most useful reporter on the effect of broadening.[34]

In Fig. 5, we plot the average position of the oscillator as a function of time for different Γ according to CME/SH and FP. We take the symmetric case, $\bar{E}_d = 0$ ($\bar{E}_d \equiv E_d - g^2/\hbar\omega$ is the renormalized energy level), so that at long times, all positions should relax to $0.5x_1$ (where x_1 is the minimum of diabat 1 and 0 is the minimum of diabat 0). We consider two separate cases.

- The nuclei are initialized to be in equilibrium with the donor diabat 1 as in Eqs. (25) and (26), so that the nuclei start off in the left well and the molecular level is occupied. See Fig. 2. This configuration is denoted "quasi equilibrium initial states" in Fig. 5.
- The nuclei are initialized in a photo-excited initial state, for which we prepare

$$P_0(x,p,0) = C\exp\Big(-\frac{1}{2}\hbar\omega(x-x_1)^2/kT_i - \frac{1}{2}\hbar\omega p^2/kT_i\Big), \tag{35}$$

$$P_1(x,p,0) = 0. \tag{36}$$

  In other words, nuclei are positioned initially in the left well (corresponding to diabat 1), even though the molecular level is unoccupied (which corresponds to diabat 0 and is minimized in the right well).

Note that, with a FP equation, one cannot distinguish these two different cases because FP equations depend only on the total nuclear density $A(x,p) = P_0(x,p) + P_1(x,p)$, and these densities are identical above.

Fig. 5 succinctly summarizes the results of this manuscript. When Γ is small, broadening does not affect the dynamics (see subplots (a) and (b)). That being said, CME and FP approaches will disagree here because $\Gamma < \hbar\omega$. Furthermore, for photo-excited initial conditions, CME trajectories reflect the dramatic effects of electronic relaxation over a long time scale while FP results cannot treat this electronic relaxation correctly.

As Γ increases, the BFP data agrees more and more with BCME/SH (see subplots (c) and (d)), since now Γ is slightly larger than ω and an adiabatic approximation is reasonable. Moreover, as Γ increases, the differences between the quasi equilibrium initial conditions and photo excited initial conditions become smaller. This convergence can be explained by recognizing that, for large Γ, electronic relaxation is swift and the remaining (slow) nuclear dynamics will occur along the unique potential of mean force.

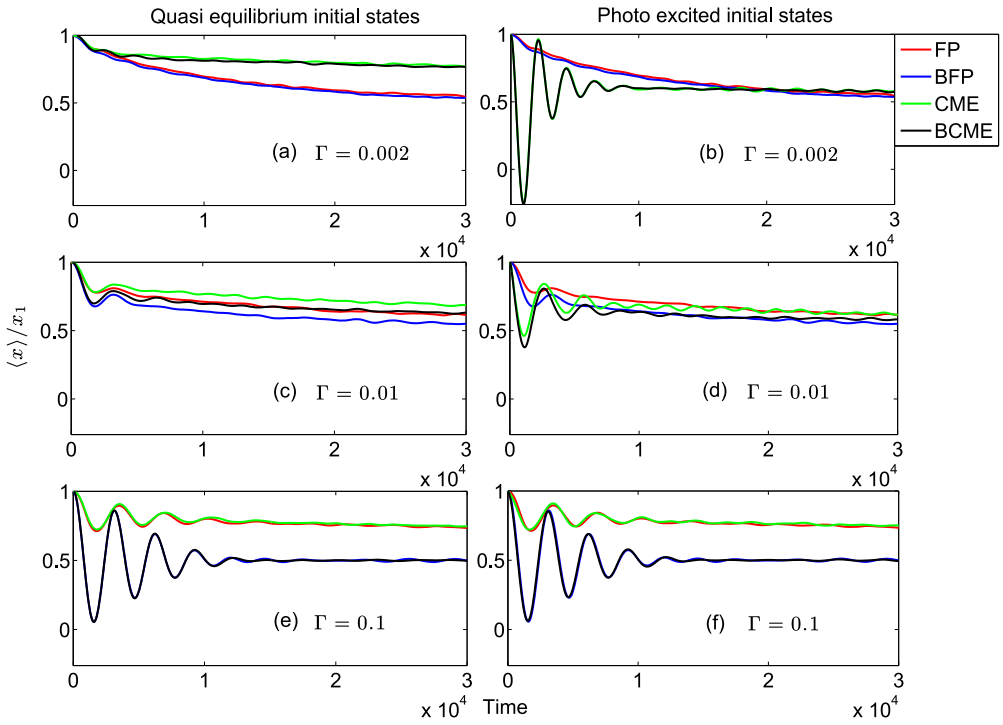

FIG. 5. Average position of the oscillator as a function of time. $\omega = 0.003$, $g = 0.015$, $kT = 0.01$, $\bar{E}_d = 0$ ($\bar{E}_d \equiv E_d - g^2/\hbar\omega$ is the renormalized energy level). We have set $\hbar = 1$. We prepare the initial temperature as $T_i = T$. x_1 corresponds to the position that minimizes the energy of the occupied diabat, $x_1 = -\sqrt{2}g/\hbar\omega$. The nuclei are initialized either to be in quasi-equilibrium with the electron (Eqs. (25) and (26)) or to be photoexcited and out of equilibrium with the electron (Eqs. (35) and (36)). Note that the BCME correctly agrees with the CME for small Γ ($\Gamma \ll kT$) and with the BFP for large Γ ($\Gamma \gg \hbar\omega$). Same notation as in Fig. 1.

Lastly we consider very large Γ in subplots (e) and (f). Here, as before, the effects of initial conditions are, of course, minimal and the FP and SH approaches agree. The interesting new feature is that, because broadening lowers the barrier between left and right wells, the dynamics on the broadened surfaces undergo large oscillations and relax rather quickly. By contrast, the unbroadened trajectories relax very slow. Note that the reorganization energy here is $E_r = g^2/\hbar\omega = 7.5\ kT$, so that the diabatic crossing point is $7.5\ kT/4 \approx 1.88\ kT$, whereas with broadening the crossing point becomes $0.6\ kT$.

There is one quirk to point out regarding the speed of relaxation. Consider the unbroadened CME/SH algorithm in subplot (b). Note that, for small Γ and photo-excited initial conditions, relaxation occurs much faster than it does for larger Γ in subplots (e) and (f). This inversion, whereby smaller Γ leads to faster relaxation, comes about because there is no direct barrier to relaxation with photo-excited initial conditions; moreover, a photo-excited electronic state will live longer with smaller Γ so that nuclei can explore more of phase space before relaxation. This realization will perhaps have fruitful consequences for modeling photo-induced electron transfer at metal surfaces.

V. CONCLUSION

In this paper, we have used a BCME to model nonadiabatic dynamics for the cases of both strong and weak molecule-metal couplings. On the one hand, in the limit of strong molecule-metal coupling, the BCME can be mapped to a BFP equation and captures level broadening correctly. On the other hand, in the limit of weak molecule-metal coupling, the BCME can be reduced to the (unbroadened) CME. Numerically, the BCME (in Eqs. (23) and (24)) can be solved easily with a SH procedure. Using such a procedure, we have shown that level broadening can affect electronic and nuclear dynamics dramatically by lowering the barrier between wells along the lower adiabatic surface. In the future, it will be crucial to benchmark this result against rigorous quantum dynamics; this research is now in progress. Furthermore, because we have introduced broadening in an *ad hoc* manner, by extrapolation, there may well be other efficient approaches that can compete with this BCME. Numerical tests will be needed. If this BCME proves as accurate and efficient as we would like, looking forward, this algorithm should be a very important tool for modeling nonadiabatic dynamics for realistic systems, e.g., scattering of gas molecules from metal surfaces[8–10] and hopefully electrochemical catalysis.[11]

ACKNOWLEDGMENTS

We thank Abe Nitzan for very useful conversations. This material is based upon work supported by the (U.S.) Air Force Office of Scientific Research (USAFOSR) PECASE award under AFOSR Grant No. FA9950-13-1-0157. J.E.S. acknowledges a Cottrell Research Scholar Fellowship and a David and Lucille Packard Fellowship.

APPENDIX A: HOW TO ACCOUNT FOR BROADENING THE ELECTRONIC FRICTION DAMPING PARAMETER

According to Ref. 26, the correctly broadened friction is of the form

$$\gamma_e^B = \frac{2g^2}{\Gamma}\frac{\omega}{kT}\mathcal{D}(E(x)), \tag{A1}$$

where we have defined

$$\mathcal{D}(Z) \equiv \Gamma \int \frac{d\epsilon}{\pi}\left(\frac{\Gamma/2}{(\epsilon - Z)^2 + (\Gamma/2)^2}\right)^2 f(\epsilon)(1 - f(\epsilon)). \tag{A2}$$

This damping parameter should be contrasted with Eq. (18).

Let us now show how we can alter our BCME in Eqs. (23) and (24) such that we match the correctly broadened electronic friction. To do so, it is important to consider two cases. First, there is the case that $\mathcal{D}(E(x)) > f(E(x))(1 - f(E(x)))$. (Below, for the sake of brevity, we do not include the inner variables $E(x)$ explicitly for $\mathcal{D}$ or f.) In such a case, one can simply include extra frictional damping (with corresponding random force) on top or our BCME.

Second, however, is the opposite case, whereby $\mathcal{D} < f(1 - f)$. In such a case, our BCME includes too much friction already. To correct this deficiency, we propose replacing the term $-\sqrt{2}gf(1 - f)\frac{\partial A(x,p,t)}{\partial p}$ in Eq. (13) by $-\sqrt{2}g\mathcal{D}\frac{\partial A(x,p,t)}{\partial p}$, and $\hbar\omega\frac{\partial f}{\partial x}pA(x,p,t)$ by $-\sqrt{2}g\frac{\hbar\omega}{kT}\mathcal{D}pA(x,p,t)$. Such a replacement will give us the correctly broadened friction from a BFP equation. Then, if we transform back from A and B to P_0 and P_1 using the definitions in Eqs. (10) and (11), we find

$$\begin{aligned}
\hbar\frac{\partial P_0(x,p,t)}{\partial t} &= -\hbar\omega p\frac{\partial P_0(x,p,t)}{\partial x} + \hbar\omega x\frac{\partial P_0(x,p,t)}{\partial p} - \Gamma f P_0(x,p,t) \\
&\quad + \Gamma(1 - f)P_1(x,p,t) + \sqrt{2}g(n - f)(1 - f)\frac{\partial\big(P_0(x,p,t) + P_1(x,p,t)\big)}{\partial p} \\
&\quad - \sqrt{2}g\frac{\hbar\omega}{kT}(\mathcal{D} - f(1 - f))p\big(P_0(x,p,t) + P_1(x,p,t)\big) \\
&\quad - \sqrt{2}g\big(\mathcal{D} - f(1 - f)\big)\frac{\partial\big(P_0(x,p,t) + P_1(x,p,t)\big)}{\partial p},
\end{aligned} \tag{A3}$$

$$\begin{aligned}
\hbar\frac{\partial P_1(x,p,t)}{\partial t} &= -\hbar\omega p\frac{\partial P_1(x,p,t)}{\partial x} + (\hbar\omega x + \sqrt{2}g)\frac{\partial P_1(x,p,t)}{\partial p} + \Gamma f P_0(x,p,t) \\
&\quad - \Gamma(1 - f)P_1(x,p,t) + \sqrt{2}g(n - f)f\frac{\partial\big(P_0(x,p,t) + P_1(x,p,t)\big)}{\partial p} \\
&\quad + \sqrt{2}g\frac{\hbar\omega}{kT}(\mathcal{D} - f(1 - f))p(P_0(x,p,t) + P_1(x,p,t)) \\
&\quad + \sqrt{2}g(\mathcal{D} - f(1 - f))\frac{\partial\big(P_0(x,p,t) + P_1(x,p,t)\big)}{\partial p}.
\end{aligned} \tag{A4}$$

Equations (A3) and (A4) can be solved via a surface hopping procedure as well. As compared with the surface hopping procedure described in Sec. III, the hopping rates now depend on both position and momentum, and we also find additional force and momentum jumps.

Of course, one might wonder: why not apply Eqs. (A3) and (A4) more generally, instead of Eqs. (23) and (24), if one wants to correctly extrapolate between the small and large Γ limits? To answer this question, we note that the new momentum jump terms are proportional to $(\mathcal{D} - (1 - f)f)/f$ (or $(\mathcal{D} - (1 - f)f)/(1 - f)$). These factors will be unstable in practice when $(\mathcal{D} - (1 - f)f) > 0$. Because of this practical limitation, if one requires the correctly broadened electronic friction, we propose switching between Eqs. (A3) and (A4) and Eqs. (23) and (24). We have found empirically that such a combination works very well.

We may now sum up this final SH algorithm.

1. Initialize all positions, momenta and active potential surfaces for all trajectories.
2. For each trajectory, if we suppose the active potential surface is 0 [or 1], we compare $\mathcal{D}$ with $(1 - f)f$.
3. If $(\mathcal{D} - (1 - f)f) > 0$, we compare $\Gamma f dt$ $[\Gamma(1 - f)dt]$ with a random number ξ in the range [0, 1].
   - If $\xi > \Gamma f dt$ $[\xi > \Gamma(1 - f)dt]$, the oscillator continues to move along potential surface 0 [surface 1] for a time step dt. In addition to the mean force F_0 $[F_1]$, the oscillator feels an extra frictional damping $\frac{2g^2}{\Gamma}\frac{\omega}{kT}(\mathcal{D} - (1 - f)f)$ and an extra random force. The mean force F_0 and F_1 are defined as

$$F_0 = -\hbar\omega x - \sqrt{2}g(n - f)f, \tag{A5}$$

$$F_1 = -\hbar\omega(x - x_1) - \sqrt{2}g(n - f)f. \tag{A6}$$

And the random force is chosen from a Gaussian distribution with variance $\sigma^2 = \frac{4g^2}{\Gamma}(\mathcal{D} - (1-f)f)/dt$.

- Otherwise, the oscillator jumps to potential surface 1 [surface 0], with the same position, and the momentum is adjusted by $-\sqrt{2}g(n-f)/\Gamma$. Thereafter, the oscillator moves for a time step dt with the mean force F_1 [F_0], extra frictional damping $\frac{2g^2}{\Gamma}\frac{\omega}{kT}(\mathcal{D} - (1-f)f)$ and an extra random force. Again, the random force is chosen from a Gaussian distribution with variance $\sigma^2 = \frac{4g^2}{\Gamma}(\mathcal{D} - (1-f)f)/dt$.

4. If $(\mathcal{D} - (1-f)f) < 0$, we compare $\bar{\gamma}_{0\to1}dt$ [$\bar{\gamma}_{1\to0}dt$] with a random number ξ in the range [0, 1], where

$$\bar{\gamma}_{0\to1} = \Gamma f + \sqrt{2}g\frac{\hbar\omega}{kT}(\mathcal{D} - f(1-f))p, \tag{A7}$$

$$\bar{\gamma}_{1\to0} = \Gamma(1-f) - \sqrt{2}g\frac{\hbar\omega}{kT}(\mathcal{D} - f(1-f))p. \tag{A8}$$

- If $\xi > \bar{\gamma}_{0\to1}dt$ [$\xi > \bar{\gamma}_{1\to0}dt$], the oscillator continues moving along potential surface 0 [surface 1] for a time step dt with the force $\bar{F}_0$ [$\bar{F}_1$], where

$$\bar{F}_0 = -\hbar\omega x - \sqrt{2}g(n-f)(1-f) + \sqrt{2}g(\mathcal{D} - f(1-f)), \tag{A9}$$

$$\bar{F}_1 = -\hbar\omega(x - x_1) - \sqrt{2}g(n-f)f - \sqrt{2}g(\mathcal{D} - f(1-f)). \tag{A10}$$

- Otherwise, the oscillator jumps to surface 1 [surface 0] with the same position but the momentum is adjusted by $\Delta p_{0\to1}$ [$\Delta p_{1\to0}$], where

$$\Delta p_{0\to1} = -\frac{\sqrt{2}g}{\Gamma}((n-f)f - \mathcal{D} + f(1-f))/f, \tag{A11}$$

$$\Delta p_{1\to0} = -\frac{\sqrt{2}g}{\Gamma}((n-f)(1-f) + \mathcal{D} - f(1-f))/(1-f). \tag{A12}$$

Thereafter, the oscillator moves for a time step dt with the force $\bar{F}_1$ [$\bar{F}_0$].

5. Repeat steps 2-4 for all trajectories until one reaches the desired final time.

APPENDIX B: MULTIPLE NUCLEAR DEGREES OF FREEDOM, BEYOND THE HARMONIC APPROXIMATION

The Hamiltonian for the case of multiple, arbitrary nuclear degrees of freedom is

$$H = H_s + H_b + H_c, \tag{B1}$$

$$H_s = E(\mathbf{X})d^+d + \sum\nolimits_i \frac{P_i^2}{2m_i} + U_0(\mathbf{X}), \tag{B2}$$

$$H_b = \sum\nolimits_k (\epsilon_k - \mu)c_k^+c_k, \tag{B3}$$

$$H_c = \sum\nolimits_k V_k(c_k^+d + d^+c_k). \tag{B4}$$

For such a Hamiltonian, the CME is

$$\begin{aligned}\frac{\partial P_0(\mathbf{X},\mathbf{P},t)}{\partial t} = &-\sum_i \frac{P_i}{m_i}\frac{\partial P_0(\mathbf{X},\mathbf{P},t)}{\partial X_i} \\ &+ \sum_i \frac{\partial U_0(\mathbf{X})}{\partial X_i}\frac{\partial P_0(\mathbf{X},\mathbf{P},t)}{\partial P_i} \\ &- \frac{\Gamma}{\hbar}f(E)P_0(\mathbf{X},\mathbf{P},t) \\ &+ \frac{\Gamma}{\hbar}(1-f(E))P_1(\mathbf{X},\mathbf{P},t),\end{aligned} \tag{B5}$$

$$\begin{aligned}\frac{\partial P_1(\mathbf{X},\mathbf{P},t)}{\partial t} = &-\sum_i \frac{P_i}{m_i}\frac{\partial P_1(\mathbf{X},\mathbf{P},t)}{\partial X_i} \\ &+ \sum_i \left(\frac{\partial E(\mathbf{X})}{\partial X_i} + \frac{\partial U_0(\mathbf{X})}{\partial X_i}\right)\frac{\partial P_1(\mathbf{X},\mathbf{P},t)}{\partial P_i} \\ &+ \frac{\Gamma}{\hbar}f(E)P_0(\mathbf{X},\mathbf{P},t) \\ &- \frac{\Gamma}{\hbar}(1-f(E))P_1(\mathbf{X},\mathbf{P},t),\end{aligned} \tag{B6}$$

where $f(E)$ is the Fermi function $f(E) = \frac{1}{e^{E(\mathbf{X})/kT}+1}$. As above, we define new densities $A(\mathbf{X},\mathbf{P},t)$ and $B(\mathbf{X},\mathbf{P},t)$,

$$P_0(\mathbf{X},\mathbf{P},t) = (1-f(E))A(\mathbf{X},\mathbf{P},t) + B(\mathbf{X},\mathbf{P},t), \tag{B7}$$

$$P_1(\mathbf{X},\mathbf{P},t) = f(E)A(\mathbf{X},\mathbf{P},t) - B(\mathbf{X},\mathbf{P},t). \tag{B8}$$

Following the same procedures as we described in Sec. II, after incorporating level broadening for the potential of mean force, we arrive at a BFP equation

$$\begin{aligned}\frac{\partial A(\mathbf{X},\mathbf{P},t)}{\partial t} = &-\sum_i \frac{P_i}{m_i}\frac{\partial A(\mathbf{X},\mathbf{P},t)}{\partial X_i} \\ &+ \sum_i \frac{\partial U(\mathbf{X})}{\partial X_i}\frac{\partial A(\mathbf{X},\mathbf{P},t)}{\partial P_i} \\ &+ \sum_{ij}\frac{\gamma_{ij}}{m_j}\frac{\partial}{\partial P_i}\left(P_jA(\mathbf{X},\mathbf{P},t)\right) \\ &+ kT\sum_{ij}\gamma_{ij}\frac{\partial^2 A(\mathbf{X},\mathbf{P},t)}{\partial P_i\partial P_j}.\end{aligned} \tag{B9}$$

Here, $U(\mathbf{X})$ is the potential of mean force,

$$\frac{\partial U(\mathbf{X})}{\partial X_i} = \frac{\partial U_0(\mathbf{X})}{\partial X_i} + n(E)\frac{\partial E(\mathbf{X})}{\partial X_i}, \tag{B10}$$

where $n(Z)$ is defined as

$$n(Z) = \int \frac{d\epsilon}{2\pi}\frac{\Gamma}{(\epsilon - Z)^2 + (\Gamma/2)^2}f(\epsilon), \tag{B11}$$

γ_{ij} is the frictional damping coefficient

$$\gamma_{ij} = \frac{\hbar}{\Gamma}\frac{1}{kT}f(E)(1-f(E))\frac{dE(\mathbf{X})}{dX_j}\frac{dE(\mathbf{X})}{dX_i}. \tag{B12}$$

Finally, we transform back to the original variables P_0 and P_1 and we find

$$\frac{\partial P_0(\mathbf{X},\mathbf{P},t)}{\partial t} = -\sum_i \frac{P_i}{m_i}\frac{\partial P_0(\mathbf{X},\mathbf{P},t)}{\partial X_i} + \sum_i \frac{\partial U_0(\mathbf{X})}{\partial X_i}\frac{\partial P_0(\mathbf{X},\mathbf{P},t)}{\partial P_i} - \frac{\Gamma}{\hbar} f(E) P_0(\mathbf{X},\mathbf{P},t)$$
$$+ \frac{\Gamma}{\hbar}(1-f(E))P_1(\mathbf{X},\mathbf{P},t) + (n(E)-f(E))(1-f(E))\sum_i \frac{\partial E(\mathbf{X})}{\partial X_i}\frac{\partial\big(P_0(\mathbf{X},\mathbf{P},t)+P_1(\mathbf{X},\mathbf{P},t)\big)}{\partial P_i}, \tag{B13}$$

$$\frac{\partial P_1(\mathbf{X},\mathbf{P},t)}{\partial t} = -\sum_i \frac{P_i}{m_i}\frac{\partial P_1(\mathbf{X},\mathbf{P},t)}{\partial X_i} + \sum_i \Big(\frac{\partial E(\mathbf{X})}{\partial X_i} + \frac{\partial U_0(\mathbf{X})}{\partial X_i}\Big)\frac{\partial P_1(\mathbf{X},\mathbf{P},t)}{\partial P_i} + \frac{\Gamma}{\hbar} f(E) P_0(\mathbf{X},\mathbf{P},t)$$
$$- \frac{\Gamma}{\hbar}(1-f(E))P_1(\mathbf{X},\mathbf{P},t) + (n(E)-f(E))f(E)\sum_i \frac{\partial E(\mathbf{X})}{\partial X_i}\frac{\partial\big(P_0(\mathbf{X},\mathbf{P},t)+P_1(\mathbf{X},\mathbf{P},t)\big)}{\partial P_i}. \tag{B14}$$

1. A correction for electronic friction

At this point, we remind the reader that Eq. (B12) does not incorporate broadening correctly. The correct friction should read

$$\gamma_{ij} = \frac{\hbar}{\Gamma}\frac{1}{kT}\mathcal{D}(E)\frac{dE(\mathbf{X})}{dX_i}\frac{dE(\mathbf{X})}{dX_j}, \tag{B15}$$

where $\mathcal{D}(Z)$ is

$$\mathcal{D}(Z) \equiv \Gamma \int \frac{d\epsilon}{\pi}\left(\frac{\Gamma/2}{(\epsilon - Z)^2 + (\Gamma/2)^2}\right)^2 f(\epsilon)(1-f(\epsilon)). \tag{B16}$$

If we want to use the prescription discussed above in Appendix A to correctly broaden the electronic friction, the corresponding CME becomes

$$\frac{\partial P_0(\mathbf{X},\mathbf{P},t)}{\partial t} = -\sum_i \frac{P_i}{m_i}\frac{\partial P_0(\mathbf{X},\mathbf{P},t)}{\partial X_i} + \sum_i \frac{\partial U_0(\mathbf{X})}{\partial X_i}\frac{\partial P_0(\mathbf{X},\mathbf{P},t)}{\partial P_i} - \frac{\Gamma}{\hbar} f(E) P_0(\mathbf{X},\mathbf{P},t) + \frac{\Gamma}{\hbar}(1-f(E))P_1(\mathbf{X},\mathbf{P},t)$$
$$+ (n(E)-f(E))(1-f(E))\sum_i \frac{\partial E(\mathbf{X})}{\partial X_i}\frac{\partial\big(P_0(\mathbf{X},\mathbf{P},t)+P_1(\mathbf{X},\mathbf{P},t)\big)}{\partial P_i}$$
$$- \sum_i \frac{1}{kT}(\mathcal{D}(E) - f(E)(1-f(E)))\frac{\partial E(\mathbf{X})}{\partial X_i}\frac{P_i}{m_i}\big(P_0(\mathbf{X},\mathbf{P},t)+P_1(\mathbf{X},\mathbf{P},t)\big)$$
$$- \sum_i \big(\mathcal{D}(E) - f(E)(1-f(E))\big)\frac{\partial E(\mathbf{X})}{\partial X_i}\frac{\partial\big(P_0(\mathbf{X},\mathbf{P},t)+P_1(\mathbf{X},\mathbf{P},t)\big)}{\partial P_i}, \tag{B17}$$

$$\frac{\partial P_1(\mathbf{X},\mathbf{P},t)}{\partial t} = -\sum_i \frac{P_i}{m_i}\frac{\partial P_1(\mathbf{X},\mathbf{P},t)}{\partial X_i} + \sum_i \Big(\frac{\partial E(\mathbf{X})}{\partial X_i} + \frac{\partial U_0(\mathbf{X})}{\partial X_i}\Big)\frac{\partial P_1(\mathbf{X},\mathbf{P},t)}{\partial P_i} + \frac{\Gamma}{\hbar} f(E) P_0(\mathbf{X},\mathbf{P},t)$$
$$- \frac{\Gamma}{\hbar}(1-f(E))P_1(\mathbf{X},\mathbf{P},t) + (n(E)-f(E))f(E)\sum_i \frac{\partial E(\mathbf{X})}{\partial X_i}\frac{\partial\big(P_0(\mathbf{X},\mathbf{P},t)+P_1(\mathbf{X},\mathbf{P},t)\big)}{\partial P_i}$$
$$+ \sum_i \frac{1}{kT}(\mathcal{D}(E) - f(E)(1-f(E)))\frac{\partial E(\mathbf{X})}{\partial X_i}\frac{P_i}{m_i}\big(P_0(\mathbf{X},\mathbf{P},t)+P_1(\mathbf{X},\mathbf{P},t)\big)$$
$$+ \sum_i \big(\mathcal{D}(E) - f(E)(1-f(E))\big)\frac{\partial E(\mathbf{X})}{\partial X_i}\frac{\partial\big(P_0(\mathbf{X},\mathbf{P},t)+P_1(\mathbf{X},\mathbf{P},t)\big)}{\partial P_i}. \tag{B18}$$

The surface hopping procedure for solving Eqs. (B13) and (B14) or Eqs. (B17) and (B18) is effectively the same as the one phonon case described in Sec. III and Appendix A. For brevity, we do not repeat the algorithm here.

[1]M. Head-Gordon and J. C. Tully, J. Chem. Phys. **103**, 10137 (1995).
[2]M. Galperin, M. A. Ratner, and A. Nitzan, J. Phys.: Condens. Matter **19**, 103201 (2007).
[3]M. Galperin, M. A. Ratner, and A. Nitzan, Nano Lett. **5**, 125 (2005).
[4]A. Nitzan, Annu. Rev. Phys. Chem. **52**, 681 (2001).
[5]M. R. Delbecq, V. Schmitt, F. D. Parmentier, N. Roch, J. J. Viennot, G. Féve, B. Huard, A. C. C. Mora, and T. Kontos, Phys. Rev. Lett. **107**, 256804 (2011).
[6]F. Cavaliere, E. Mariani, R. Leturcq, C. Stampfer, and M. Sassetti, Phys. Rev. B **81**, 201303(R) (2010).
[7]K. F. Albrecht, A. Martin-Rodero, R. C. Monreal, L. Mühlbacher, and A. L. Yeyati, Phys. Rev. B **87**, 085127 (2013).
[8]N. Shenvi, S. Roy, and J. C. Tully, J. Chem. Phys. **130**, 174107 (2009).
[9]N. Shenvi, S. Roy, and J. C. Tully, Science **326**, 829 (2009).

[10]Y. Huang, C. T. Rettner, D. J. Auerbach, and A. M. Wodtke, Science **290**, 111 (2000).
[11]W. Ouyang, J. G. Saven, and J. E. Subotnik, J. Phys. Chem. C **119**, 20833 (2015).
[12]P. W. Anderson, Phys. Rev. **124**, 41 (1961).
[13]T. Holstein, Ann. Phys. **8**, 325 (1959).
[14]In fact, for this model problem, we can list three more energy scales: the reorganization energy for the nuclear degree of freedom (E_r, which is proportional to the electron-phonon coupling g, $E_r = g^2/(\hbar\omega)$), the energy difference between the occupied and unoccupied level (E_d), and the bandwidth of the metal W.
[15]A. C. Hewson and D. Meyer, J. Phys.: Condens. Matter **14**, 427 (2002).
[16]R. Bulla, T. A. Costi, and T. Pruschke, Rev. Mod. Phys. **80**, 395 (2008).
[17]K. G. Wilson, Rev. Mod. Phys. **47**, 773 (1975).
[18]M. Thoss, I. Kondov, and H. Wang, Phys. Rev. B **76**, 153313 (2007).
[19]L. Mühlbacher and E. Rabani, Phys. Rev. Lett. **100**, 176403 (2008).
[20]W. Dou, A. Nitzan, and J. E. Subotnik, J. Chem. Phys. **142**, 084110 (2015).
[21]F. Elste, G. Weick, C. Timm, and F. von Oppen, Appl. Phys. A **93**, 345 (2008).
[22]J. Koch, F. von Oppen, Y. Oreg, and E. Sela, Phys. Rev. B **70**, 195107 (2004).
[23]W. Dou, A. Nitzan, and J. E. Subotnik, J. Chem. Phys. **142**, 234106 (2015).
[24]L. Siddiqui, A. W. Ghosh, and S. Datta, Phys. Rev. B **76**, 085433 (2007).
[25]R. Härtle and M. Thoss, Phys. Rev. B **83**, 125419 (2011).
[26]N. Bode, S. V. Kusminskiy, R. Egger, and F. von Oppen, Beilstein J. Nanotechnol. **3**, 144 (2012).
[27]M. Thomas, T. Karzig, S. V. Kusminskiy, G. Zaránd, and F. von Oppen, Phys. Rev. B **86**, 195419 (2012).
[28]M. Brandbyge, P. Hedegård, T. F. Heinz, J. A. Misewich, and D. M. Newns, Phys. Rev. B **52**, 6042 (1995).
[29]D. Mozyrsky, M. B. Hastings, and I. Martin, Phys. Rev. B **73**, 035104 (2006).
[30]W. Dou, A. Nitzan, and J. E. Subotnik, J. Chem. Phys. **143**, 054103 (2015).
[31]M. Galperin and A. Nitzan, J. Phys. Chem. Lett. **6**(24), 4898 (2015).
[32]J. C. Tully, J. Chem. Phys. **93**, 1061 (1990).
[33]W. Dou, A. Nitzan, and J. E. Subotnik, "Molecular electronic states near metal surfaces at equilibrium using potential of mean force and numerical renormalization group methods: Hysteresis revisited," J. Chem. Phys. (submitted).
[34]There is one important nuance here, however. We find that, for large electron phonon couplings, the effect of broadening the frictional parameter can be very important and easily measured by plotting the average kinetic energy (or many other observables as well). For the present BCME algorithm, however, our SH protocol does not broaden the friction; in general, we presume that there will usually be other sources of friction that might swamp out such effects. Nevertheless, see Appendix A for a detailed approach regarding how such broadening may be implemented.